Driven diffusion in the two-dimensional lattice Coulomb gas: A model for flux flow in superconducting networks

Jong-Rim Lee
Center for Theoretical Physics, Seoul National University, Seoul 151-742, Republic of Korea

S. Teitel
Department of Physics and Astronomy, University of Rochester, Rochester, New York 14627
(Received 2 December 1993)

We carry out driven-diffusion Monte Carlo simulations of the two-dimensional classical lattice Coulomb gas in an applied uniform electric field, as a model for vortex motion due to an applied dc current in a periodic superconducting network. A finite-size version of dynamic scaling is used to extract the dynamic critical exponent z, and infer the nonlinear response at the transition temperature. We consider the Coulomb gases $f = 0$ and $f = 1/2$, corresponding to a superconducting network with an applied transverse magnetic field of zero, and one-half flux quantum per unit cell, respectively.

I. INTRODUCTION

Phase transitions in two dimensional (2D) superconducting networks, such as periodic Josephson junction arrays and superconducting wire nets, has been a topic of much investigation.[1] Theoretically, the phase transitions in such systems have been most extensively studied by *equilibrium* calculations and simulations.[2–7] Experimentally however, it has been most common to measure steady-state current-voltage (I-V) characteristics, and look for a crossover from linear to nonlinear resistivity as a signal of the superconducting transition.[8,9] In this regard, the Kosterlitz-Thouless (KT) model[10] of a vortex pair unbinding transition makes a clear prediction:[11,12] as one heats up through the transition temperature $T_{\rm KT}$, the I-V characteristics should make a discontinuous change from $V \sim I^3$ exactly at $T_{\rm KT}$ to $V \sim I$ above $T_{\rm KT}$. In experimental studies of superconducting 2D films[13] and networks[9] however, as well as in numerical simulations,[14] agreement with this prediction has been claimed in some cases, not found in others, and is ambiguous in yet others. In particular, it is not clear how this prediction may become modified when a transverse magnetic field is applied to the sample. In this case, the melting of the ground state vortex lattice induced by the magnetic field may change the universality class of the superconducting transition, and lead to different steady-state behavior. In view of these questions, it remains of interest to establish what steady-state I-V behavior may be expected at criticality, for specific simple cases.

Recently, a new dynamic scaling conjecture was proposed by Fisher *et al.*[15] to describe I-V characteristics in superconducting systems. Although this approach was developed for application to the "vortex-glass" transition in high temperature superconductors, it should apply equally well to any superconducting transition that is believed to be second order. In this work we carry out steady-state "driven-diffusion" Monte Carlo (MC) simulations[16] of the 2D lattice Coulomb gas[4,5] in a uniform applied electric field, as a model for vortex motion due to a uniform applied dc current, in a periodic superconducting network. We consider the special cases of $f = 0$, corresponding to no transverse magnetic field, and $f = 1/2$, corresponding to a transverse magnetic field of one-half flux quantum per unit cell of the network. We apply a finite-size version of the new dynamic scaling conjecture to analyze our data, and extract the dynamic critical exponent z, and the power law of the I-V characteristic at the superconducting transition. For $f = 0$, we find $z = 2$, consistent with the Kosterlitz-Thouless prediction. For $f = 1/2$, we again find $z = 2$, consistent with the KT model, but in disagreement with expectations from recent equilibrium simulations of this model.

The remainder of this paper is organized as follows. In Sec. II, we give the theoretical framework for our simulations. We present our Coulomb gas model and the driven-diffusion Monte Carlo algorithm. We review the KT vortex pair unbinding prediction, and we describe the finite-size version of dynamic scaling. In Sec. III, we present our numerical results for $f = 0$ and for $f = 1/2$. In Sec. IV, we give our conclusions.

II. THEORETICAL FRAMEWORK

A. The driven diffusive lattice Coulomb gas

The standard model[2,3] to describe behavior in a 2D superconducting network, is the uniformly frustrated 2D XY model, given by the Hamiltonian,

$$\mathcal{H}_{XY} = \sum_{\langle ij \rangle} U(\theta_i - \theta_j - A_{ij}). \tag{1}$$

0163-1829/94/50(5)/3149(9)/$06.00

Here θ_i is the phase of the superconducting wave function at node i of the periodic network, the sum is over all nearest neighbor bonds $\langle ij \rangle$ of the network, and

$$A_{ij} = \frac{2e}{\hbar c} \int_i^j \mathbf{A} \cdot d\boldsymbol{l} \tag{2}$$

is the line integral of the magnetic vector potential $\mathbf{A}$ across the bond from i to j. For a uniform magnetic field applied transverse to the plane of the network, the sum of the A_{ij} around (going counter clockwise) any unit cell is,

$$\sum_{\text{cell}} A_{ij} = 2\pi f, \qquad f = B\mathcal{A}/\Phi_0, \tag{3}$$

where $\mathcal{A}$ is the area of a unit cell, and the constant f is the density of magnetic flux quanta ($\Phi_0 = 2e/hc$) per unit cell. f is referred to as the "uniform frustration". $U(\phi)$ is the interaction potential between the nodes of the network, which is periodic in ϕ with period 2π, and has a minimum at $\phi = 0$. For a Josephson junction array, one takes[17] $U(\phi) = -J_0 \cos(\phi)$. For a wire net, the Villain,[18] or "periodic Gaussian" interaction may be more appropriate.[19]

It is generally believed that it is the excitation of vortices in the superconducting phase θ_i that is responsible for the superconducting transition in such networks.[2] Since 2D vortices interact with a logarithmic potential,[10] the Hamiltonian (1) is assumed to be in the same universality class (for the Villain interaction,[18] the mapping via duality is exact[20]) as the following Hamiltonian for Coulomb interacting point charges,

$$\mathcal{H}_{\text{CG}} = \tfrac{1}{2} \sum_{ij} (n_i - f) V(\mathbf{r}_i - \mathbf{r}_j)(n_i - f). \tag{4}$$

Here, i and j label the *dual* sites of the original superconducting network, $n_i = 0, \pm 1, \pm 2, \ldots$ is the integer vorticity of the superconducting phase θ at site i, CG denotes Coulomb gas, and $V(\mathbf{r})$ is the 2D lattice Green's function, which satisfies,

$$\Delta^2 V(\mathbf{r}_i - \mathbf{r}_j) = -2\pi \delta_{ij}, \tag{5}$$

where Δ^2 is the discrete Laplacian. In this work we restrict our interest to a square network, with periodic boundary conditions. In this case, $V(\mathbf{r})$ is explicitly given by

$$V(\mathbf{r}) = \frac{1}{N} \sum_{\mathbf{k}} e^{i\mathbf{k}\cdot\mathbf{r}} \frac{\pi}{2 - \cos k_x - \cos k_y}, \tag{6}$$

where $\mathbf{k}$ are the allowed wave vectors with $k_\mu = (2\pi n_\mu / L)$, with $n_\mu = 0, 1, \ldots, L-1$. L is the length of the network, and $N = L^2$. For large $\mathbf{r}$,

$$V(\mathbf{r}) \sim \ln r. \tag{7}$$

Since $V(\mathbf{r} = \mathbf{0})$ is divergent, the partition sum over $\{n_i\}$ is restricted to neutral configurations where

$$\frac{1}{N} \sum_i n_i = f. \tag{8}$$

See Ref. 5 for further details. Thus the average density of vortices is equal to the density of flux quantum of the applied magnetic field.

The Hamiltonian (4), therefore, represents a density f of integer point charges, on a uniform compensating background charge $-f$, interacting with the 2D Coulomb potential. For $f = 0$, the ground state is the vacuum, and low lying excitations are bound neutral pairs of $n_i = \pm 1$. For $f = 1/2$, the ground state is an ordered checkerboard lattice of charges[3] with $n_i = +1$ on every other site, as shown in Fig. 1. Low lying excitations may be viewed either as a displacement of one of the charges in the ground state lattice, or equivalently the creation of a neutral $\Delta n_i = \pm 1$ pair of charges superimposed on the ground state lattice configuration. It is this Coulomb gas analog of the superconducting network that we will use to carry out our simulations.

To model flux flow resistance in the superconducting network, we apply a uniform electric field to the Coulomb gas charges n_i; this models the uniform Magnus force[17] that an applied dc current exerts on vortices in the superconductor. The net charge current density in the Coulomb gas then corresponds to the net vortex current density in the superconductor, which is proportional to the net flux flow electric field (or voltage drop per unit length) in the superconductor. If we denote as $\mathbf{E}$ the applied electric field, and $\mathbf{J}$ the resulting charge current density, in the Coulomb gas analog, and $\mathcal{J}$ the applied dc current density, and $\mathcal{E}$ the resulting flux flow electric field, in the superconducting network, then the correspondence between the models is given by

$$\mathbf{E} \leftrightarrow \mathcal{J}, \qquad \mathbf{J} \leftrightarrow \mathcal{E}. \tag{9}$$

The simulation of the Coulomb gas in the presence of the uniform $\mathbf{E}$ is carried out by use of the driven-diffusion technique.[16] We imagine adding to the Hamiltonian (4) the term

$$\delta\mathcal{H} = -\sum_i n_i \mathbf{r}_i \cdot \mathbf{E} \tag{10}$$

which represents a dipole interaction between the charges n_i and the electric field $\mathbf{E}$. Although $\mathcal{H}_{\text{CG}} + \delta\mathcal{H}$ is unbounded, and, therefore, not a valid Hamiltonian in a global sense, when it is used as a *local* energy function

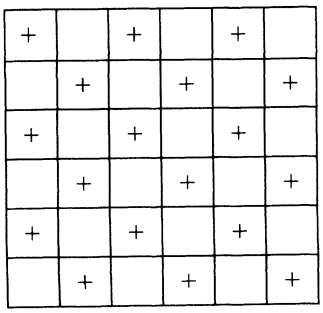

FIG. 1. Ground state charge lattice for the $f = 1/2$ Coulomb gas. A + denotes the presence of a charge $n_i = +1$.

for computing energy differences, in connection with the standard Metropolis Monte Carlo algorithm for accepting or rejecting proposed excitations, it yields an enhanced probability (consistent with detailed balance) for accepting excitations with a net movement of charge in the direction of $\mathbf{E}$, thus setting up a nonequilibrium steady-state with a finite charge current density $\mathbf{J}$ flowing parallel to $\mathbf{E}$.

In our simulations, we have chosen $\mathbf{E} = E\hat{y}$, along one of the axes of the periodic lattice of sites. At each step of the simulation we pick at random a pair of nearest neighbor sites (i_0, i_1). For the $f = 0$ case (where the ground state is $n_i = 0$), we add a positive unit charge to site i_0, i.e., $\Delta n_{i_0} = +1$, and a negative unit charge to site i_1, i.e., $\Delta n_{i_1} = -1$. For the $f = 1/2$ case (where the ground state is as in Fig. 1), we simply interchange the charges n_{i_0} and n_{i_1} at the two sites. For $f = 1/2$, this restricts configurations to those where half of the n_i are $+1$ and the other half are 0; charges $n_i = -1$ or $+2$ are not allowed. Tests showed that these other values of n_i correspond to higher energy excitations, which are negligible at the temperatures of interest, i.e., the melting temperature of the ground state charge lattice. In both the $f = 0$ and the $f = 1/2$ cases, the change in energy due to the addition of the excitation is computed using $\mathcal{H}_{CG} + \delta\mathcal{H}$, and the excitation is accepted or rejected using the Metropolis algorithm. In both cases, acceptance of the excitation gives a contribution to the average current density,

$$\Delta\mathbf{J} = \Delta n_{i_0}\frac{\mathbf{r}_{i_0} - \mathbf{r}_{i_1}}{2} + \Delta n_{i_1}\frac{\mathbf{r}_{i_1} - \mathbf{r}_{i_0}}{2} = \Delta n_{i_0}(\mathbf{r}_{i_0} - \mathbf{r}_{i_1}), \tag{11}$$

where Δn_i is the change in n_i at site i created by adding the excitation, and our algorithm always satisfies $\Delta n_{i_0} = -\Delta n_{i_1}$.

While the above driven-diffusion Monte Carlo algorithm encodes a specific dynamics, which in detail may well be different from the true microscopic dynamics of vortices in superconductors, our hope is that qualitative behaviors which are largely determined by energetics, particularly the nonlinear form at criticality, will be preserved. We have chosen[21] to simulate the driven-diffusion Coulomb gas, rather than the more realistic resistively shunted junction (RSJ) model[17] for the dynamics of an array of Josephson junctions[14,22], because in the Coulomb gas algorithm one directly moves the important degrees of freedom, the positions of the vortices. This results in a computationally faster algorithm for several reasons: (i) spin wave degrees of freedom are eliminated; (ii) the effective energy barrier for an isolated vortex to hop to a neighboring cell in the XY model[12] is removed, since in the Coulomb gas this hop takes place in one discrete step; (iii) the RSJ dynamics requires a computation of order L^2 (or $L \ln L$ for improved algorithms[23]) at each step of simulation. For the Coulomb gas, where we keep tabulated the "electrostatic potential" arising from the charges,[4] computing the energy of a trial excitation is a computation of order 1. Only when an excitation is accepted, and we need to update this electrostatic potential, do we have to do a computation of order L^2. For the low acceptance ratios we find, this effect is significant.[5]

$N = L^2$ steps of the above updating process will be referred to a one MC pass. In our runs, presented in Sec. III, an initial 10 000 passes were typically discarded to equilibrate the system. Following this equilibration, five independent runs (using different random number sequences) of 200 000 passes each, were used to compute averages. Our error bars are estimated from the standard deviation of the averages from these five runs.

B. Kosterlitz-Thouless pair unbinding model

We now review the Kosterlitz-Thouless model of pair unbinding,[10,13] as applied to the determination of nonlinear steady-state behavior[11] below the transition temperature T_{KT}. If we consider the addition of a neutral pair of charges $\Delta n_i = \pm 1$ separated by a distance $\mathbf{r}$, we may estimate the free energy of this pair in the presence of all other charges as,

$$F_{\text{pair}}(\mathbf{r}) = \frac{1}{\epsilon}(\ln|\mathbf{r}| - \mathbf{E}\cdot\mathbf{r}). \tag{12}$$

Here ϵ is the effective long wavelength dielectric function of the Coulomb gas, which serves to screen the logarithmic interaction between the members of the pair, as well as to screen the interaction of the pair with the external field $\mathbf{E}$. A pair oriented along the direction of $\mathbf{E}$, therefore, sees a potential maximum at $r_c = 1/E$. If the pair is able to overcome this potential barrier through thermal fluctuations, the pair can then lower its free energy by increasing the separation r without bound. The pair will thus unbind, and give a contribution to a net current of charges flowing along the direction of $\mathbf{E}$. The rate for such critical pair unbindings to occur is given by the Boltzmann factor,

$$W_{\text{pair}} \sim e^{-F_{\text{pair}}(r_c)/T} \sim E^{1/\epsilon T}. \tag{13}$$

Such critical pairs will expand until they recombine with other such free charges into new bound pairs. This unbinding and recombination of pairs leads[11] to an effective density of free charges n_f,

$$n_f \sim (W_{\text{pair}})^{1/2}. \tag{14}$$

Using Eqs. (13) and (14), the net current that flows due to pair unbinding is then,

$$J \sim n_f E \sim E^{1+1/2\epsilon T}. \tag{15}$$

The insulator to metal transition in the Coulomb gas, where ϵ diverges, marks the crossover from nonlinear to linear J-E characteristics. Using the correspondence of Eq. (9), together with $I = L\mathcal{J}$ and $V = L\mathcal{E}$ for the total current and total voltage drop in a superconducting network, we see that this Coulomb gas insulator to metal transition corresponds to the superconducting to normal transition in the superconducting network.

For $f = 0$, where the ground state is the vacuum,

pair unbinding excitations such as above, are believed to be the only source of net charge current. The Kosterlitz-Thouless model is expected to describe the insulator to metal transition in this system, and gives the prediction[10,13] that $\epsilon^{-1}(T)$ has a universal discontinuous jump to zero exactly at the transition temperature $T_{\rm KT}$, with,

$$1/\epsilon(T_{\rm KT})T_{\rm KT} = 4. \tag{16}$$

Thus, exactly at $T_{\rm KT}$, Eq. (15) gives the nonlinear behavior, $J \sim E^3$. The corresponding result in the superconducting network is $V \sim I^3$.

For $f = 1/2$, where the ground state is the doubly degenerate ordered charge lattice shown in Fig. 1, the above pair unbinding continues to provide a mechanism for nonlinear response below the insulator to metal transition temperature, which we will continue to refer to as $T_{\rm KT}$. However, there are now also other possible excitations, involving the formation of domains of oppositely oriented ground state, which might possibly contribute[14] to a nonlinear response in J. Thus no clear prediction exists for the form of the nonlinear response at the transition.

Similarly, the nature of the *equilibrium* transition in the $f = 1/2$ model remains controversial.[3,4,6,7] If $T_{\rm KT}$ is the insulator to metal transition, the Kosterlitz-Thouless arguments continue to provide a lower bound on a discontinuous jump in ϵ^{-1}, i.e., $1/\epsilon(T_{\rm KT})T_{\rm KT} \geq 4$. It is unclear however, whether this is satisfied only as an inequality, or whether the universal KT behavior as in Eq. (16) continues to hold. Additionally, there is a well defined temperature T_M in the model, corresponding to the melting of the ordered ground state charge lattice. General arguments[24] suggest the bound $T_M \geq T_{\rm KT}$, however it remains unclear whether or not these two temperatures are in fact equal. It is further unclear whether the melting transition at T_M is Ising-like (as the double discrete symmetry of the ground state suggests), or whether the long range interactions between the charges cause the melting to fall in a new universality class. Our present work was in part motivated by the hope that dynamic calculations might shed some light on these remaining equilibrium questions.

C. Finite-size dynamic scaling

Recently, Fisher *et al.*[15] have proposed the following dynamic scaling relation, for an infinite superconducting system with a second order phase transition at T_c. The relation between the dissipative electric field $\mathcal{E}$, and the applied dc current density $\mathcal{J}$, is given by,

$$\mathcal{E} = \mathcal{J}\xi^{d-2-z}\Phi_{\pm}(\mathcal{J}\xi^{d-1}/T), \tag{17}$$

where ξ is the spatial correlation length, d the dimensionality of the system, z the dynamic scaling exponent, and $\Phi_{\pm}$ the scaling function above and below the transition. The most natural generalization of this form, to a system of finite length L, is,

$$\mathcal{E} = \mathcal{J}b^{d-2-z}\Phi(\mathcal{J}b^{d-1}/T, tb^{1/\nu}, b/L), \tag{18}$$

where b is an arbitrary length rescaling factor, $t = (T - T_c)/T_c$, and ν is the correlation length scaling exponent, $\xi \sim t^{-\nu}$. The form Eq. (17) can be obtained from Eq. (18) by choosing $b = \xi$, and taking $L \to \infty$. For finite L, Φ is a continuous function as t passes through zero. Only in the $L \to \infty$ limit does $\Phi(\mathcal{J}, t, 0)$ become discontinuous as t passes through zero; this determines the different scaling functions Φ_+ and Φ_- of Eq. (17).

From Eq. (18) one can now determine the scaling behavior at criticality, $t = 0$. Choosing $b = \mathcal{J}^{-1/(d-1)}$, $L \to \infty$, and setting $t = 0$, one finds,

$$\mathcal{E} = \mathcal{J}^{1-(d-2-z)/(d-1)}\Phi(1/T_c, 0, 0) \sim \mathcal{J}^{(1+z)/(d-1)}, \tag{19}$$

as found by Fisher *et al.*[15] Thus at T_c, one always expects a nonlinear power law response. For $d = 2$, a dynamic exponent of $z = 2$ recovers the $\mathcal{E} \sim \mathcal{J}^3$ result of the KT pair unbinding picture.

Using the correspondences of Eq. (9), we now recast the scaling Eq. (18) into a form for use with our Coulomb gas model. Choosing the rescaling length $b = L$, we get,[25]

$$J = EL^{d-2-z}\Phi(EL^{d-1}/T, tL^{1/\nu}, 1). \tag{20}$$

Finally, for $d = 2$, exactly at criticality, $t = 0$, we have the scaling,

$$J = EL^{-z}\Phi(EL/T_c, 0, 1). \tag{21}$$

To fit this scaling equation to our Monte Carlo data, and extract the dynamic exponent z, we use the method used by Nightingale and Blöte[26] for similar equilibrium problems. We consider behavior exactly at T_c, as a function of varying E, in the limit of large L but small EL. Expanding the scaling function Φ gives,

$$J(E, L) = EL^{-z}[\Phi_0 + \Phi_1 EL + \Phi_2(EL)^2 + O(EL)^3]. \tag{22}$$

Truncating this expansion at any finite order, we perform a least χ^2 nonlinear fit[27] of our Monte Carlo data to Eq. (22) to determine the unknown parameters z, and the Φ_i.

We check for stability of our fit by increasing the order of the expansion, and by dropping data from successively smaller values of L, and checking if the fitted parameters change within our estimated statistical error. Statistical errors in the fitted parameters are estimated by generating many synthetic data sets, by adding random noise to each of the original MC data point. The noise for each data point is taken from a Gaussian distribution whose width is set equal to the estimated statistical error of the original MC data point. Using these fictitious data sets, we repeat the fitting procedure to obtain new fitted parameters. The estimated error of a parameter is then taken as the standard deviation of the results from all the fictitious data sets.

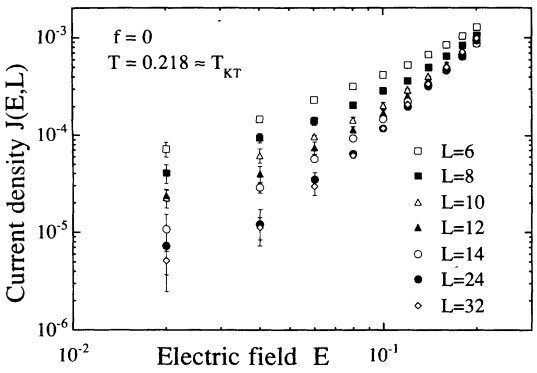

FIG. 2. Charge current density $J(E, L)$ versus applied electric field E for various square lattice sizes L, at fixed temperature $T_{\rm KT} = 0.218$, for the $f = 0$ model. 10^6 total MC passes were used to compute averages.

III. NUMERICAL RESULTS

A. $f = 0$

For our simulations of the $f = 0$ Coulomb gas, corresponding to the ordinary XY model, we use as the equilibrium KT transition temperature $T_{\rm KT} = 0.218$, as determined by one of us[28] from a finite-size scaling analysis applied to equilibrium simulations of $\epsilon^{-1}(T, L)$. This value is in good agreement with earlier estimates, based on Coulomb gas simulations by Saito and Müller-Krumbhaar,[29] $T_{\rm KT} = 0.215$, and by Grest,[4] $T_{\rm KT} = 0.220$. In Fig. 2, we plot the resulting charge current density $J(E, L)$ versus E, for several values of L, at the fixed temperature $T_{\rm KT} = 0.218$. We see that the smaller E, the larger is the finite-size effect as L varies. From Eq. (21) we see that smaller values of E probe larger length scales; correspondingly, our statistical error increases as E decreases.

To find the dynamic exponent z, we now fit the data of Fig. 2 to the expanded scaling function of Eq. (22). Since this expansion converges fastest for small values of the argument, we restrict the data used in our fitting to those points where $EL \leq 1$. This corresponds to lattice sizes $L = 6 - 14$, with $E = 0.02 - 0.08$. In Table I, we show the results of this fit, for several orders of expansion, for various ranges of L. Using the fourth order expansion for lattice sizes $L = 8 - 14$, we find $z = 2.073 \pm 0.098$. Using this z in Eq. (19), we get a nonlinear response $J \sim E^{3.073}$, consistent with the prediction from the KT pair unbinding model, assuming the universal jump in $\epsilon^{-1}(T_{\rm KT})$ [see Eqs. (15) and (16)].

In Fig. 3, we plot our data as JL^z/E versus EL. We see that the data collapse onto a universal curve

TABLE I. Results of the fitting of J to an expansion of the scaling function in powers of EL, as in Eq. (22). The data of Fig. 2 for the $f = 0$ model is used. The first column shows the range of system sizes $L_i - L_f$ which are included in the particular fit. The following columns give the fitted parameters. The last column is the χ^2 error of the fit. For each sequence of $L_i - L_f$, the first row gives the value of the fitted parameter, while the second row gives the estimated error.

$L_i - L_f$	z	Φ_0	Φ_1	Φ_2	Φ_3	Φ_4	$\chi^2_{\rm fit}$
			First order expansion				
6 – 14	1.9831	0.1017	0.0935				8.8463
	0.0590	0.0106	0.0215				
8 – 14	2.0297	0.1070	0.1148				6.5589
	0.1097	0.0261	0.0459				
10 – 14	2.0777	0.1119	0.1415				5.0160
	0.1382	0.0393	0.0535				
			Second order expansion				
6 – 14	2.0067	0.1281	0.0137	0.0734			4.8485
	0.0663	0.0253	0.0740	0.0733			
8 – 14	2.0747	0.1541	0.0040	0.0995			3.6025
	0.1163	0.0524	0.1058	0.1038			
10 – 14	2.1203	0.1657	0.0195	0.1053			2.9278
	0.1238	0.0677	0.1284	0.1079			
			Third order expansion				
6 – 14	2.0060	0.1268	0.0192	0.0631	0.0052		4.8474
	0.0953	0.0345	0.1114	0.1335	0.1307		
8 – 14	2.0725	0.1520	0.0132	0.0835	0.0077		3.6012
	0.1075	0.0373	0.0940	0.1105	0.1159		
10 – 14	2.1208	0.1669	0.0131	0.1174	-0.0065		2.9228
	0.1220	0.0525	0.1906	0.2496	0.1196		
			Fourth order expansion				
6 – 14	2.0101	0.1219	0.0076	0.0790	0.0068	-0.0061	4.8552
	0.0722	0.0290	0.0693	0.1261	0.0545	0.0170	
8 – 14	2.0727	0.1517	0.0144	0.0789	0.0151	-0.0040	3.5949
	0.0984	0.0284	0.0928	0.1073	0.0694	0.0491	
10 – 14	2.1175	0.1638	0.0227	0.0966	0.0115	-0.0064	2.9201
	0.0980	0.0304	0.0825	0.1252	0.0455	0.0400	

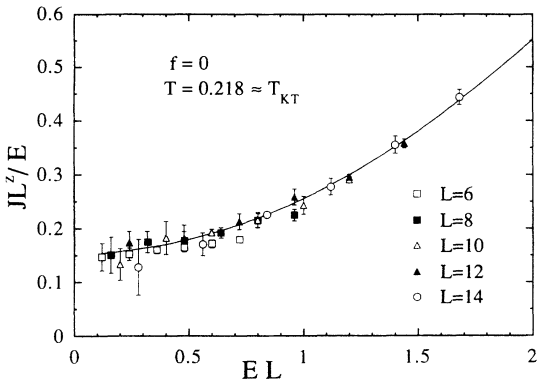

FIG. 3. The finite-size scaling behavior of the charge current density. JL^z/E versus EL is plotted for various system sizes L at fixed temperature $T_{\rm KT} = 0.218$, for the $f = 0$ model. Symbols with error bars represent the MC data. The solid line results from the fitting to Eq. (22) using a fourth order expansion in EL, and data from $L = 8 - 14$ and $E = 0.02 - 0.08$. Data from $E = 0.1$ and 0.12 for each lattice size are included in the plot. The fitted value of $z = 2.073$ was used in making the vertical axis. 10^6 total MC passes were used to compute averages.

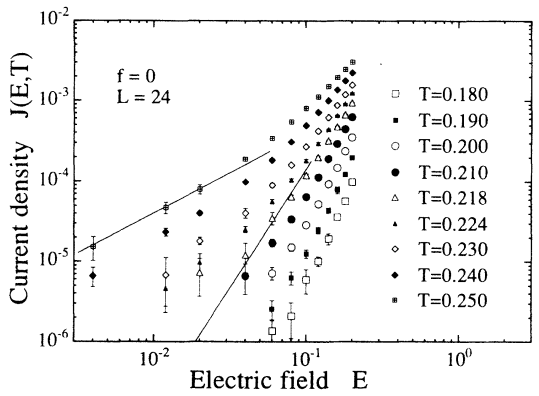

FIG. 4. Charge current density $J(E,T)$ versus E for various temperatures T, for fixed system size $L = 24$, for the $f = 0$ model. The solid lines from left to right have slopes 1 and 3, respectively, illustrating Ohmic behavior above $T_{\rm KT}$, and KT critical behavior at $T_{\rm KT}$. 10^6 total MC passes were used to compute averages.

representing the scaling function $\Phi(x, 0, 1)$. The value $z = 2.073$, obtained from the fitting, is used in making the vertical axis, and the solid line is drawn using the fitted values of the Φ_i. Although the agreement is reasonable, Table I does suggest some potential problems. The parameters $z \simeq 2$ and Φ_0, while remaining stable within the estimated errors, both show a systematic increase as the smallest L_i used in the fit is increased. Φ_2, although consistent within the different fits, shows a very large estimated statistical error (other Φ_i, although also strongly fluctuating, seem too small to be significant in the fit). Ideally, one would like to carry out these fits using increasingly smaller values of E than we have used here. However, when E becomes small, equilibration times become large, and we were unable to get accurate enough data to improve our fit.

Our results in Table I and Fig. 3 represent checks of scaling in the small EL limit. We have also tried to check scaling in the large EL limit. Provided that EL is sufficiently large that finite-size effects are small, we should be able to use Eq. (17) to collapse our data onto two universal curves, given by Φ_+ and Φ_- above and below $T_{\rm KT}$, by plotting $J\xi^z/E$ versus $E\xi/T$. To do so, we need an expression for the correlation length $\xi(T)$. For the Kosterlitz-Thouless transition, asymptotically close to $T_{\rm KT}$, this form is,[10,13]

$$\xi_\pm(T) \sim e^{C_\pm/|T-T_{\rm KT}|^\nu}, \qquad (23)$$

where the subscripts + and − refer to behavior above and below $T_{\rm KT}$, respectively, and for the KT transition, $\nu = 1/2$. Minnhagen and Olsson[30] have argued that this true asymptotic form holds only in a narrow critical region of about 5% of $T_{\rm KT}$. Nevertheless, they also indicate that Eq. (23) is a useful phenomenological form for fitting over a wider temperature range for $T > T_{\rm KT}$, provided C_+ is taken as a phenomenological parameter not necessarily equal to the true asymptotic value. We adopt this approach and use Eq. (23) with $C_\pm$ and ν as phenomenological parameters.

To carry out this large EL check of scaling, we observe from our data at $T_{\rm KT}$ in Fig. 2, that finite-size effects are negligible provided we restrict the data to $L \geq 24$, $E \geq 0.06$. Since this is true at $T_{\rm KT}$, it should also certainly be true for other values of T. We, therefore, carry out simulations on an $L = 24$ lattice, for values $E \geq 0.14$. Our results for $J(E,T)$ versus E, for various T above and below $T_{\rm KT}$, are shown in Fig. 4 on a log-log scale. Solid lines with slopes of 1 (for Ohmic behavior above $T_{\rm KT}$), and 3 (for critical behavior at $T_{\rm KT}$) are shown for reference. In Fig. 5, we try to collapse this data onto two universal curves as discussed above, by finding the best choices for the parameters $T_{\rm KT}$, z, $C_\pm$, and ν. The results shown are for the values $T_{\rm KT} = 0.218$, $z = 2$ (consistent with our small EL analysis), $\nu = 1/2$ (consistent with the KT form), and $C_+ = C_- = 0.35$. We have found that this collapse is very sensitive to the value of $T_{\rm KT}$;

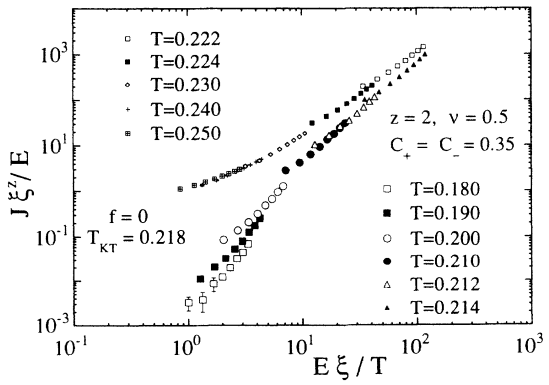

FIG. 5. Test of the infinite-size scaling relation Eq. (17) for the $f = 0$ model. The data of Fig. 4 is replotted as $J\xi^z/E$ versus $E\xi/T$, using the form of Eq. (23) to determine $\xi(T)$. Parameters z, $T_{\rm KT}$, ν, and $C_\pm$ are varied, to get the best collapse of the data onto two distinct scaling functions $\Phi_\pm$, above and below $T_{\rm KT}$.

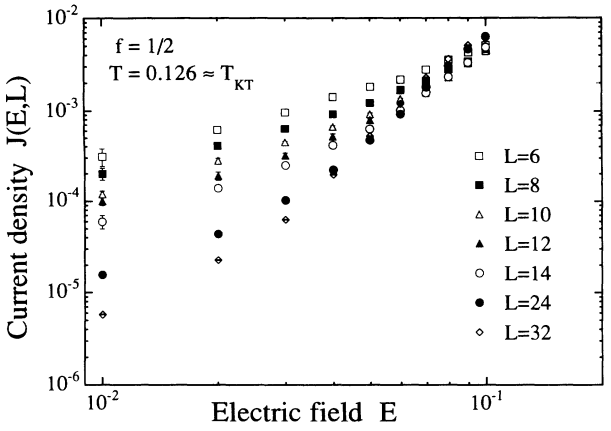

FIG. 6. Charge current density $J(E,L)$ versus applied electric field E for various square lattice sizes L, at fixed temperature $T_{\rm KT} = 0.126$, for the $f = 1/2$ model. 10^6 total MC passes were used to compute averages.

when $T_{\rm KT}$ is varied only 1%, the data for different T fail to overlap at all. When either z, ν, or $C_\pm$ are varied by more than roughly 10%, the quality of the collapse decreases substantially. There is no apparent reason that our fitted parameters satisfy $C_+ = C_-$. The collapse appears reasonable for $T > T_{\rm KT}$, but is much less so for $T < T_{\rm KT}$, particularly at the smallest several values of T. This is most likely due to a failure of the assumed form for $\xi(T)$, Eq. (23), to be valid over such a large temperature range, as well as to poor equilibration at the smallest values of E (in Fig. 4, we see that for $T < T_{\rm KT}$, the raw data points for the smallest E appear to curve slightly upwards to somewhat higher J than one might expect from the shape of the rest of these curves).

B. $f = 1/2$

In this section, we carry out a similar analysis as in the previous section, except applied to the $f = 1/2$ Coulomb gas, which corresponds to the "fully frustrated" XY model. As discussed at the end of Sec. II B, there are in principle two transitions in this model: a insulator to metal transition at $T_{\rm KT}$, and a charge lattice melting transition at T_M. It is $T_{\rm KT}$ that corresponds to the transition from nonlinear to linear $J - E$ characteristics [see Eq. (15) and following discussion]. The most recent equilibrium simulations of the $f = 1/2$ Coulomb gas model by one of us[6] find that $T_{\rm KT} \simeq 0.126$ is very close to, but slightly below $T_M \simeq 0.1315$; the discontinuous jump in ϵ^{-1} is $1/\epsilon(T_{\rm KT})T_{\rm KT} \simeq 5.35$, larger than the universal KT value of 4 [see Eq. (16)]. This compares with ear-

TABLE II. Results of the fitting of J to an expansion of the scaling function in powers of EL, as in Eq. (22). The data of Fig. 6 for the $f = 1/2$ model are used. The first column shows the range of system sizes $L_i - L_f$ which are included in the particular fit. The following columns give the fitted parameters. The last column is the χ^2 error of the fit. For each sequence of $L_i - L_f$, the first row gives the value of the fitted parameter, while the second row gives the estimated error.

$L_i - L_f$	z	Φ_0	Φ_1	Φ_2	Φ_3	Φ_4	$\chi^2_{\rm fit}$
			First order expansion				
6 – 14	1.8976	0.7788	1.3337				14.2661
	0.0869	0.1134	0.6810				
8 – 14	1.9556	0.8891	1.5631				12.3852
	0.0954	0.1659	0.8506				
10 – 14	1.9894	0.9327	1.7894				10.5980
	0.0591	0.0573	0.6560				
			Second order expansion				
6 – 14	1.9158	0.9092	0.6484	1.1746			11.2051
	0.0921	0.1706	0.6392	0.6416			
8 – 14	2.0622	1.4525	-0.2034	3.4457			4.5429
	0.1233	0.5364	0.5575	2.7420			
10 – 14	2.1514	1.8426	-0.5706	4.8902			3.0757
	0.0680	0.2814	0.9038	1.7059			
			Third order expansion				
6 – 14	1.9128	0.8566	1.2388	-0.9075	2.0827		11.0736
	0.0938	0.2125	1.0552	3.6274	3.5002		
8 – 14	2.0602	1.3639	0.7936	0.0519	3.3454		4.3721
	0.1246	0.3867	1.8768	4.4841	6.9044		
10 – 14	2.1581	1.6954	1.5878	-2.4100	7.3724		2.5403
	0.0699	0.2873	1.0701	1.8182	5.3878		
			Fourth order expansion				
6 – 14	1.9125	0.8636	1.0860	0.0985	-0.4950	2.1906	11.0117
	0.0896	0.1444	0.9954	1.7584	2.9752	3.0877	
8 – 14	2.0597	1.3482	0.8797	0.3090	1.4246	2.2639	4.3701
	0.1238	0.4363	0.9554	1.1924	2.0356	5.9653	
10 – 14	2.1554	1.6883	1.3351	-0.2117	1.0093	5.6638	2.5421
	0.0821	0.3368	1.3246	1.9165	1.6536	6.1369	

lier estimates by Grest[4] of $T_{KT} = 0.129 \pm 0.002$, with a jump $1/\epsilon(T_{KT})T_{KT} \simeq 4.88 \pm 0.31$. Similar simulations on the fully frustrated XY model by Ramirez-Santiago and José[7] find $T_{KT} \approx T_M$ and a jump $1/\epsilon(T_{KT})T_{KT} \simeq 5.21$.

Fixing the temperature at $T_{KT} = 0.126$, we show in Fig. 6 our results for $J(E,L)$ versus E for various L. To extract the critical exponent z we fit this data to the expanded scaling function of Eq. (22). We restrict[31] the data used in our fitting to those points where $EL \leq 0.5$, which corresponds to lattice sizes $L = 6 - 14$, with $E = 0.01 - 0.04$. In Table II, we show the results of this fit. Using the fourth order expansion for lattice sizes $L = 8 - 14$, we find $z = 2.060 \pm 0.124$. As was found for $f = 0$, the result $z \simeq 2$ is consistent with a power law response of $J \sim E^3$.

In Fig. 7 we plot the data of Fig. 6 as JL^z/E versus EL, and find fair agreement with the expected collapse onto a universal curve. Our fitted value of $z = 2.060$ is used in making the vertical axis, and the solid line is drawn using the fitted values of the Φ_i. Although the agreement is reasonable, Table II again suggests some potential problems. As we found in Table I for the $f = 0$ case, now for $f = 1/2$, the parameters z and Φ_0 show a systematic increase as the smallest L_i used in the fit is increased. Now however, this increase is more pronounced, and the fitted values remain consistent with varying L_i only within the outer limits of the estimated statistical errors. Furthermore, the higher Φ_i all seem to be significant, and all have very large statistical error. These observations make it unclear whether or not our data truly represents the asymptotic scaling region of large L, small EL.

We have not attempted to check scaling for this $f = 1/2$ model in the large EL limit. The strong finite-size effects seen in Fig. 6, even comparing $L = 24$ and 32, means that we would have to go either to larger lattice sizes (which are beyond our present computational ability), or to temperatures sufficiently far from T_{KT}, in order to reach the large EL limit, for the values of E we have studied. Uncertainties in the correct form one should take for $\xi(T)$, due in particular to the close proximity of the vortex lattice melting transition at T_M to the insulator to metal transition at T_{KT}, would undoubtedly make such an analysis more complicated than was the case for $f = 0$.

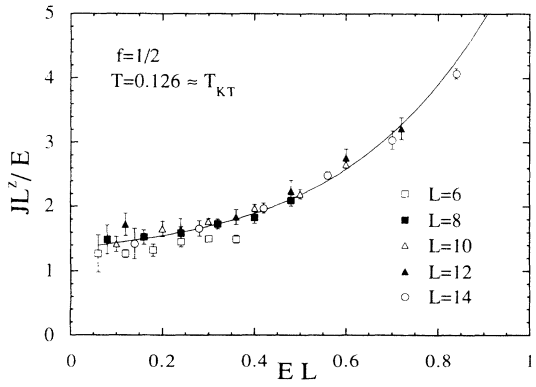

FIG. 7. The finite-size scaling behavior of the charge current density. JL^z/E versus EL is plotted for various system sizes L at fixed temperature $T_{KT} = 0.126$, for the $f = 1/2$ model. Symbols with error bars represent the MC data. The solid line results from the fitting to Eq. (22) using a fourth order expansion in EL, and data from $L = 8 - 14$ and $E = 0.01 - 0.04$. Data from $E = 0.05$ and 0.06 for each lattice size are included in the plot. The fitted value of $z = 2.060$ was used in making the vertical axis. 10^6 total MC passes were used to compute averages.

IV. CONCLUSIONS

To conclude, we have carried out steady-state driven-diffusion Monte Carlo simulations of the 2D lattice Coulomb gas, in order to compute the dynamic exponent z, and hence obtain the nonlinear response $J \sim E^a$, $a = z+1$, at criticality. This corresponds to the nonlinear current-voltage characteristic $V \sim I^a$ in a superconducting network at the superconducting to normal transition. We have analyzed our data according to a finite-size scaling method based on a new dynamic scaling conjecture by Fisher *et al.*[15]

For the $f = 0$ model, corresponding to a superconducting network in zero applied magnetic field, our results agree with the familiar Kosterlitz-Thouless pair unbinding model. Our finite-size scaling analysis, varying L and E at fixed $T = T_{KT}$, gives a value of $z \simeq 2$, consistent with a power law response at T_{KT} of $a = 3$. Our check of scaling in the infinite L limit, where we vary T and E for fixed L large, shows fair agreement with the Kosterlitz-Thouless model, but success is limited by our limited knowledge of the form of the correlation length $\xi(T)$ outside the narrow critical region.

For the $f = 1/2$ model, corresponding to a superconducting network in an applied magnetic field of one-half flux quantum per unit cell, we again find $z \simeq 2$. This is consistent with the Kosterlitz-Thouless pair unbinding result of Eq. (15) only if the discontinuous jump in $\epsilon^{-1}(T_{KT})$ obeys the universal KT prediction of Eq. (16), i.e., $1/\epsilon(T_{KT})T_{KT} = 4$. Equilibrium simulations[6] however indicate that for $f = 1/2$, this jump is nonuniversal, with $1/\epsilon(T_{KT})T_{KT} \simeq 5.35$. Using this value of ϵ in Eq. (15) yields the nonlinear response at T_{KT} due to pair unbinding as, $J \sim E^a$, with $a = 3.68$. If pair unbinding were the dominant contribution to J, this would imply a dynamic exponent of $z = a - 1 = 2.68$. This conclusion is based on energetic considerations alone, and hence is not influenced by our particular choice of Monte Carlo dynamics, versus a more realistic microscopic superconductor dynamics.

It remains unclear what is the source of this inconsistency. It could be that the analysis[6] of ϵ^{-1} in the equilibrium simulations is in error; this equilibrium analysis involves identifying leading logarithmic corrections at T_{KT} which may be hard to determine accurately. Or it could be that our finite-size analysis of z in this present work is flawed; this possibility is indicated by the less than satisfactory behavior of the fitted parameters (see Table II, and discussion at the end of Sec. III B) as we vary the order of the fitting expansion, or the system sizes used

in the fit. Or it could be that the result $z = 2$ is a more general property of such superconducting systems, which is independent of the KT pair unbinding model; in this case one would expect that some excitation other than pairs gives the dominant contribution to J at T_{KT}. The natural guess for these other excitations is the domain excitations of the ground state charge lattice. However, this would seem unlikely if the charge lattice melting transition T_M is distinctly higher than T_{KT}, as equilibrium simulations suggest. Therefore, behavior in the $f = 1/2$ model remains an enigma, both from the equilibrium, and now from the steady-state dynamic point of view.

ACKNOWLEDGMENTS

This work has been supported by U. S. Department of Energy Grant No. DE-FG02-89ER14017, and in part by the Korea Science and Engineering Foundation through the SRC program of SNU-CTP.

[1] For a recent review see, Proceedings of the NATO Advanced Research Workshop on Coherence in Superconducting Networks, Delft, 1987, edited by J. E. Mooij and G. B. J. Schön [Physica **142**, 1 (1988)].

[2] S. Teitel and C. Jayaprakash, Phys. Rev. Lett. **51**, 1999 (1983); W. Y. Shih and D. Stroud, Phys. Rev. B **20**, 6774 (1984); **32**, 158 (1985); T. C. Halsey, J. Phys. C **18**, 2437 (1985); S. E. Korshunov and G. V. Umin, J. Stat. Phys. **43**, 1 (1986); S. E. Korshunov, *ibid.* **43**, 17 (1986); J. P. Straley, Phys. Rev. B **38**, 11 225 (1984).

[3] S. Teitel and C. Jayaprakash, Phys. Rev. B **27**, 598 (1983); S. Miyashita and H. Siba, J. Phys. Soc. Jpn. **53**, 1145 (1984); D. H. Lee, J. D. Joannopolos, J. W. Negele, and D. P. Landau, Phys. Rev. B **33**, 450 (1986); J. M. Thijssen and H. J. F. Knops, *ibid.* **37**, 7738 (1988); H. Eikmans, J. E. van Himbergen, H. J. F. Knops, and J. M. Thijssen, *ibid.* **39**, 11 759 (1989); D. B. Nicolaides, J. Phys. A **24**, L231 (1991); J. Lee, J. M. Kosterlitz, and E. Granato, Phys. Rev. B **43**, 11 531 (1991); E. Granato, J. M. Kosterlitz, J. Lee, and M. P. Nightingale, Phys. Rev. Lett. **66**, 1090 (1991).

[4] G. S. Grest, Phys. Rev. B **39**, 9267 (1989).

[5] J.-R. Lee and S. Teitel, Phys. Rev. B **46**, 3247 (1992).

[6] J.-R. Lee, Phys. Rev. B **49**, 3317 (1994).

[7] G. Ramirez-Santiago and J. V. José, Phys. Rev. Lett. **68**, 1224 (1992).

[8] J. Resnick, J. C. Garland, J. T. Boyd, S. Shoemaker, and R. S. Newrock, Phys. Rev. Lett. **47**, 1542 (1981); R. F. Voss and R. A. Webb, Phys. Rev. B **25**, 3446 (1982); D. W. Abraham, C. J. Lobb, M. Tinkham, and T. M. Klapwijk, **26**, 5268 (1982); R. K. Brown and J. C. Garland, *ibid.* **33**, 7827 (1986); C. W. Wilks, R. Bojko, and P. M. Chaikin, *ibid.* **43**, 2721 (1991); F. Yu, N. E. Israeloff, and A. M. Goldman, Phys. Rev. Lett. **68**, 2535 (1992).

[9] B. J. van Wees, H. S. J. van der Zant, and J. E. Mooij, Phys. Rev. B **35**, 7291 (1987); J. P. Carini, *ibid.* **38**, 63 (1988); H. S. J. van der Zant, M. N. Webster, J. Romijn, and J. E. Mooij, *ibid.* **42**, 2647 (1990); H. S. J. van der Zant, H. A. Rijken, and J. E. Mooij, J. Low Temp. Phys. **79**, 289 (1990); **82**, 67 (1991).

[10] J. M. Kosterlitz and D. Thouless, J. Phys. C **6**, 1181 (1973); J. M. Kosterlitz, *ibid.* **7**, 1046 (1974); A. P. Young, *ibid.* **11**, L453 (1978).

[11] B. I. Halperin and D. R. Nelson, J. Low Temp. Phys. **36**, 599 (1979); V. Ambegaokar, B. I. Halperin, D. R. Nelson, and E. D. Siggia, Phys. Rev. B **21**, 1806 (1980).

[12] C. J. Lobb, D. W. Abraham, and M. Tinkham, Phys. Rev. B **27**, 150 (1983).

[13] P. Minnhagen, Rev. Mod. Phys. **59**, 1001 (1987).

[14] K. K. Mon and S. Teitel, Phys. Rev. Lett. **62**, 673 (1989).

[15] D. S. Fisher, M. P. A. Fisher, and D. A. Huse, Phys. Rev. B **43**, 130 (1991).

[16] S. Katz, J. L. Lebowitz, and H. Spohn, Phys. Rev. B **28**, 1655 (1983); J. Stat. Phys. **34**, 497 (1984); J. S. Wang, K. Binder, and J. L. Lebowitz, *ibid.* **56**, 783 (1989). For a review see, B. Schmittmann, Int. J. Mod. Phys. B **4**, 2269 (1990).

[17] M. Tinkham, *Introduction to Superconductivity* (McGraw-Hill, New York, 1975).

[18] J. Villain, J. Phys. (Paris) **36**, 581 (1975).

[19] S. Teitel and C. Jayaprakash, J. Phys. (Paris) Lett. **46**, L-33 (1985).

[20] J. V. José, L. P. Kadanoff, S. Kirkpatrick, and D. R. Nelson, Phys. Rev. B **16**, 1217 (1977); R. Savit, *ibid.* **17**, 1340 (1978); E. Fradkin, B. Huberman, and S. Shenker, *ibid.* **18**, 4789 (1978).

[21] While this work was being completed, we learned of similar computations being carried out, for $f = 0$, by H. Weber and M. Wallin (unpublished). These authors also consider the effects of random pinning potentials on the steady-state response.

[22] J. S. Chung, K. H. Lee, and D. Stroud, Phys. Rev. B **40**, 6570 (1989); F. Falo, A. R. Bishop, and P. S. Lomdahl, *ibid.* **41**, 10983 (1990); Y.-H. Li and S. Teitel, Phys. Rev. Lett. **65**, 2595 (1990), **67**, 2894 (1991); P. L. Leath and W. Xia, Phys. Rev. B **44**, 9619 (1991).

[23] H. Eikmans and J. E. van Himbergen, Phys. Rev. B **41**, 8927 (1990).

[24] B. Nienhuis, in *Phase Transitions and Critical Phenomena*, edited by C. Domb and J. Leibowitz (Academic, London, 1987), Vol. 11, p. 1.

[25] Similar approaches have been used in, K. H. Lee and D. Stroud, Phys. Rev. B **45**, 2417 (1992); M. Wallin and S. M. Girvin, *ibid.* **47**, 14642 (1993); K. H. Lee, D. Stroud, and S. M. Girvin, *ibid.* **48**, 1233 (1993).

[26] M. P. Nightingale and H. W. Blöte, Phys. Rev. Lett. **60**, 1562 (1988).

[27] We use the Levenberg-Marquart method. See, W. H. Press, B. Flannery, S. A. Teukolsky, and W. T. Vetterling, *Numerical Recipes* (Cambridge University Press, Cambridge, 1986), pp. 521-528.

[28] J.-R. Lee, Ph. D. thesis, University of Rochester, 1993.

[29] Y. Saito and H. Müller-Krumbhaar, Phys. Rev. B **23**, 308 (1981).

[30] P. Minnhagen and P. Olsson, Phys. Rev. B **45**, 10 557 (1992).

[31] We chose a smaller limit for EL, as compared to our fits for $f = 0$, because (as we will see in Table II) even with this smaller limit, the higher order coefficients Φ_i are more significant for $f = 1/2$ than for $f = 0$.